CHARACTERIZATION OF AMORPHOUS SILICATE AND ORGANIC BEARING MIXTURES IN ANTICIPATION OF THE OSIRIS-REx ARRIVAL AT BENNU. K. L. Donaldson Hanna[1], L. P. Keller[2], D. L. Schrader[3], T. J. McCoy[4], N. E. Bowles[1], N. M. Johnson[5], J. A. Nuth[5], G. D. Cody[6], H. C. Connolly Jr.[7], L. F. Lim[5] and D. S. Lauretta[8], [1]University of Oxford (Kerri.DonaldsonHanna@physics.ox.ac.uk), [2]Johnson Space Center, [3]Arizona State University, [4]Smithsonian Institution, [5]Goddard Spaceflight Center, [6]Carnegie Institution for Science, [7]Rowan University, and [8]University of Arizona.

Introduction: NASA's Origins, Spectral Interpretation, Resource Identification, and Security-Regolith Explorer (OSIRIS-REx) mission successfully launched on September 8th, 2016. During its rendezvous with near-Earth asteroid (101955) Bennu beginning in 2018, OSIRIS-REx will characterize the asteroid's physical, mineralogical, and chemical properties to globally map these properties of Bennu, a primitive carbonaceous asteroid, and choose a sampling location [e.g., 1, 2]. In preparation for these observations, we characterized a suite of analog samples bearing synthesized insoluble organic material (IOM) and Fe- and Mg-rich amorphous silicate smokes. Here we present transmission electron microscopy (TEM) analyses of the amorphous silicate samples and thermal infrared (TIR) laboratory measurements of the analog sample suite measured under asteroid-like conditions, which are relevant to the interpretation of spectroscopic observations by the OSIRIS-REx Thermal Emission Spectrometer (OTES) [3].

Analog Samples: Analog samples in this study include physical mixtures with increasing amounts of amorphous silicates and IOM. A base physical mixture was made of olivine (77.8 wt.%), pyroxene (11.1 wt.% of which 9.4 wt.% was low-Ca pyroxene and 1.7 wt.% was high-Ca pyroxene) and plagioclase (11.1 wt.%). Additional physical mixtures include: (1) 95 wt.% base mixture + 5 wt.% amorphous material, (2) 95 wt.% (95 wt.% base mixture + 5 wt.% amorphous material) + 5 wt.% IOM, (3) 80 wt.% base mixture + 20 wt.% amorphous material and (4) 80 wt.% (80 wt.% base mixture + 20 wt.% amorphous material) + 20 wt.% IOM. The amorphous material was mixed in the proportions to match the Fe/Mg ratio determined for amorphous silicates in carbonaceous chondrites (60 wt.% Fe and 40 wt.% Mg [e.g., 4]). We also characterized the Mg-amorphous silicate and Fe-amorphous silicate smokes as pure end members. We prepared mineral end members and physical mixtures similarly to those described in [5]. The Smithsonian Mineral and Meteorites Collection (SMCC) and Arizona State University (ASU) Center for Meteorite Studies provided the well-characterized minerals. Further discussion of the IOM and amorphous silicate smokes can be found in [5-7; respectively].

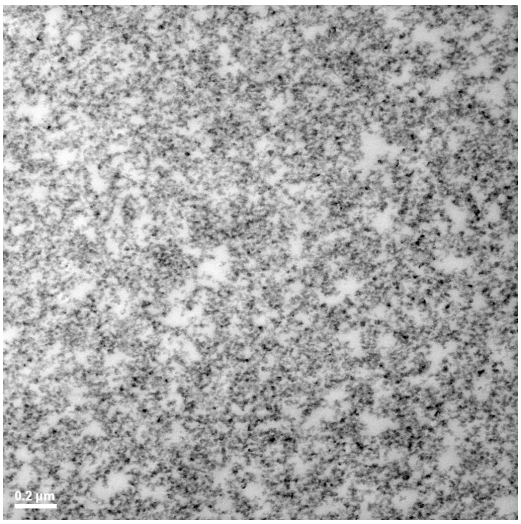

Figure 1. A brightfield TEM image of the Fe-rich amorphous silicate sample showing the typical fractal aggregate texture.

Experimental Methods: We analyzed the amorphous silicate end members using the transmission electron microscope to characterize the physical nature of the samples and measured all physical mixtures and amorphous silicate end members across TIR wavelengths for spectral characterization.

TEM: We embedded aliquots of the amorphous silicate samples in low viscosity epoxy and prepared thin sections for TEM analyses by ultramicrotomy. We performed the TEM analyses in the Electron Beam Analysis Labs at NASA/JSC.

TIR Spectroscopy: We made TIR emissivity measurements under Earth-like (ambient) and simulated asteroid environment (SAE) conditions using the Simulated Lunar Environment Chamber (SLEC) within the Planetary Spectroscopy Facility at the University of Oxford. The experimental setup and calibration of SLEC have been previously described by Thomas et al. [8, 9]. Under ambient conditions, samples are heated from below to 80°C while holding the environment chamber at ambient pressure (~1000 mbar N_2) and temperature (~28°C). The thermal gradient experienced in the upper hundreds of microns in Bennu's regolith, is simulated by: (1) removing atmospheric gases from inside the chamber (< 10^{-4} mbar), (2) cooling the interior of the chamber to < -150°C, and (3)

heating the samples from below and above until the maximum brightness temperature of the sample is ~75°C. Thermal infrared spectra were collected using a Bruker IFS66v Fourier Transform Infrared (FTIR) spectrometer at a resolution of 4 cm^{-1} from ~2400 – 400 cm^{-1} (~4 – 25 μm).

Previous lab measurements of Bennu analogs including physical mixtures and chondritic meteorites demonstrated the importance of making TIR spectral measurements under the appropriate near-surface conditions (simulated thermal gradient) as observed changes to spectral features were dependent on meteorite type [10]. While CR, CI and ordinary chondrites behave spectrally similar to pure minerals and lunar soils [e.g., 11-12], CM and CV chondrites have unique spectral behavior including the enhancement of features near 10 μm.

Results: The Fe-rich amorphous silicate sample consists of fractal aggregates of ~0.1 μm grains and is compositionally homogeneous (Fig. 1). The Mg-rich sample shows similar textures, but is partly recrystallized/annealed and contains abundant carbonaceous coatings.

Emissivity spectra measured under SAE conditions in Fig. 2 show the utility of TIR spectral features for characterizing the effects of increasing amounts of amorphous silicates and IOM. The addition of 5 wt.% amorphous silicates reduces the strength of the fundamental vibration bands (also known as the reststrahlen bands or RB) between ~1150 – 850 cm^{-1} and ~700 – 400 cm^{-1} and the transparency features (TF; emissivity minima near 800 cm^{-1} and at wavenumbers > 1300 cm^{-1}). No significant change in the position of the Christiansen feature (CF; emissivity maximum near ~1250 cm^{-1}) is observed. The addition of 5 wt.% IOM further reduces the strength of the RB and TF. Further reductions in the RB and TF are seen in the physical mixtures that include 20 wt.% amorphous silicates and 20 wt.% IOM (Fig. 2). The addition of 20 wt.% amorphous material shifts the CF to higher wavenumbers while the addition of 20 wt.% IOM causes the CF to widen and lose spectral contrast.

Discussion: Across much of the TIR spectral range, the only observed changes related to the addition of amorphous silicates and IOM are differences in the contrast of spectral features. Other factors including albedo, particle size, porosity and the near surface environment are also known to change the contrast of these features [e.g., 10-12], thus the observed changes to the spectra cannot be uniquely related to the addition of IOM and amorphous materials. However, a subtle feature near 1400 cm^{-1} is observed with the addition of amorphous silicates and IOM. Further investigation is needed to assess whether this feature can be used to uniquely identify amorphous silicates and IOM in TIR spectra.

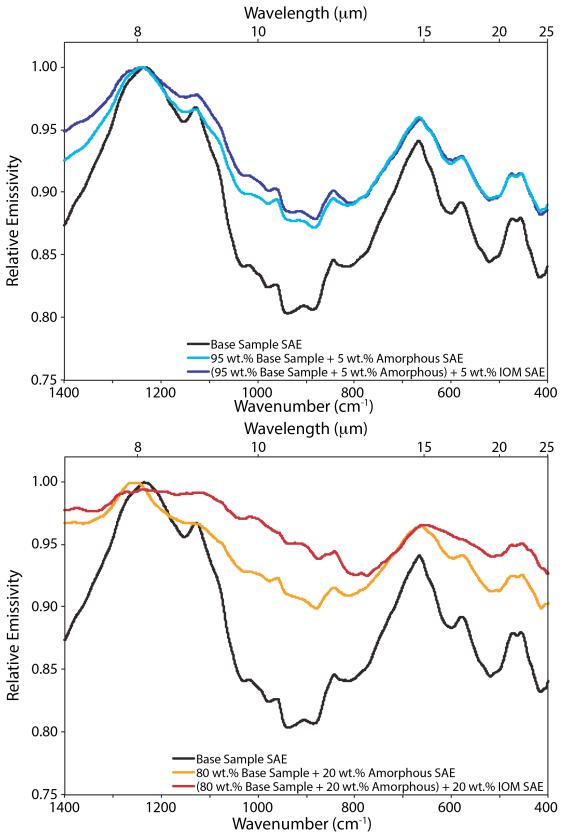

Figure 2. (Top) Spectra of the base physical mixture along with physical mixtures that include 5 wt.% amorphous materials and 5 wt.% IOM. **(Bottom)** Spectra of the base physical mixture along with physical mixtures that include 20 wt.% amorphous materials and 20 wt.% IOM.

Acknowledgements: This work is supported by NASA under contract NNM10AA11C issued through the New Frontiers Program. We thank the SI and ASU for the samples used in this study. Donaldson Hanna thanks the UK Space Agency for their support.

References: [1] Lauretta D. S. et al. (2015) *Meteoritics & Planet. Sci., 50,* 834-849. [2] Lauretta D. S. et al. (2017) *Space Sci. Rev., 212*, 925-984. [3] Christensen P. R. et al. (2017) arXiv preprint arXiv:1704.02390. [4] Le Guillou C. (2015) *EPSL* 420, 162-173. [5] Cody G. D. et al. (2011) *PNAS, 108*, 19171. [6] Schrader D. L. et al. (2017) *LPS XLVIII*, Abstract #1273. [7] Hallenbeck S. L. et al. (1998) Icarus 131, 198-209. [8] Thomas I. R. et al. (2012) *Rev. Sci. Instrum., 83*(12), 124502. [9] Thomas I. R. et al. (2014) *LPS XLV*, Abstract #1989. [10] Donaldson Hanna K. L. et al. (2017) *LPS XLVIII*, Abstract #1723. [11] Logan L. M. et al. (1973) *JGR, 78*, 4983-5003. [12] Donaldson Hanna K. L. et al. (2017) *Icarus, 283*, 326-342.